

SCIENTIFIC DATA




OPEN

DATA DESCRIPTOR

A comprehensive database of active and potentially-active continental faults in Chile at 1:25,000 scale

Valentina Maldonado^{1,2}, Martín Contreras¹ & Daniel Melnick^{1,2}  

In seismically-active regions, mapping active and potentially-active faults is the first step to assess seismic hazards and site selection for paleoseismic studies that will estimate recurrence rates. Here, we present a comprehensive database of active and potentially-active continental faults in Chile based on existing studies and new mapping at 1:25,000 scale using geologic and geomorphic criteria and digital elevation models derived from TanDEM-X and LiDAR data. The database includes 958 fault strands grouped into 17 fault systems and classified based on activity (81 proved, 589 probable, 288 possible). The database is a contribution to the world compilation of active faults with applications among others in seismic hazard assessments, territorial planning, paleoseismology, geodynamics, landscape evolution processes, geothermal exploration, and in the study of feedbacks between continental deformation and the plate-boundary seismic cycle along subduction zones.

Background & Summary

Despite the fact that geologists have been mapping active faults for more than a century^{1,2}, the unexpected rupture of unknown or unmapped faults during recent large-magnitude earthquakes emphasizes our limited knowledge of the location and seismic potential of tectonically-active continental structures. During the past decade, at least five moment magnitude (M_w) > 6 earthquakes have ruptured unknown continental faults. The 2010 Pichilemu, 2010 Darfield, 2011 Christchurch, 2016 Kaikoura, and 2019 Ridgecrest events involved ruptures on either completely concealed faults or unmapped fault strands^{3–7}. These earthquakes highlight the need to identify and map active faults at detail scales as a first step in the assessment of seismic hazards associated with continental faults. In addition to environmental and seismic hazards, land-use and territorial planning, and civil protection emergency management, mapping active continental faults and classifying them into fault systems is important for different disciplines in earth sciences. These include: the evaluation of coastline migration and erosion; the exploration and exploitation of groundwater, geothermal, and other energy resources; the study of landscape evolution and the underlying erosive and tectonic mechanisms; and the search for feedback mechanisms between the seismic cycle of plate-boundary faults and continental deformation along subduction zones.

Active fault databases have been used for a broad range of applications in earth sciences. The primary application has been the assessment of seismic hazards⁸, which involves interpreting surface fault traces in terms of 3D seismic sources at depth^{9–11}. Further applications have been, for example, assessing anthropogenic factors in triggered and induced seismicity¹² such as stress changes to the crust caused by hydroelectric reservoirs, underground gas storage, groundwater pumping, or fracking^{13,14}. Many geothermal fields occur in tectonically-active regions and maps of active faults have been used both for exploration and selection of drilling sites^{15,16} as well as for reservoir modelling during exploitation^{17,18}. Active fault databases have been also used in studies of volcano-tectonic interactions and structural control on volcanism in rifts¹⁹ and arcs²⁰, in the interpretation of present-day stress indicators^{21,22} as well as to infer sources of pre-instrumental earthquakes²³ and the response of groundwater to near and farfield earthquakes²⁴. Analyses of the rupture mechanism, propagation and kinematics of many recent earthquakes and earthquake sequences have relied on databases of active faults derived from geomorphic and geologic data to interpret subsurface observations and develop conceptual models^{3,6,25,26}.

¹Instituto de Ciencias de la Tierra, TAQUACH, Universidad Austral de Chile, Valdivia, Chile. ²Millennium Nucleus The Seismic Cycle Along Subduction Zones, Valdivia, Chile. e-mail: daniel.melnick@uach.cl

Since the advent of modern instrumental seismology, earthquakes in Chile have accounted for >20% of the seismic moment release on Earth. The earthquakes accounted for in this estimate occurred along the megathrust fault that limits the Nazca and South American plates. However, the South American continental plate, as most upper-plates along subduction zones, includes numerous active faults, some associated with $M_w > 6$ earthquakes. Interestingly, the historical record of such *continental* earthquakes in Chile is relatively small, including only seven instrumentally-recorded events of M_w between 6 and 7 (Refs. 4,27–29). Out of these, only two (2001 Aroma and 2007 Aysén) occurred on mapped faults; another two were directly associated with larger earthquakes on the underlying plate-boundary megathrust (2010 Pichilemu and 2014 Pisagua) but occurred on unmapped faults. Only a few paleoseismic trenching studies have been carried out along four Chilean continental faults finding robust evidence for $M_w > 6$ paleoearthquakes^{30,31}. It is however expected that the activity of further faults will be verified during forthcoming paleoseismic mapping and trenching endeavours. Recurrence periods of continental earthquakes estimated from paleoseismic and seismological studies are in the range of thousands of years (an order of magnitude larger than recurrence periods of megathrust earthquakes); nevertheless, considering the incipient knowledge of Chilean continental faults and their widespread spatial distribution, the seismic hazards posed by such structures should not be underestimated.

Research initiatives on active faults in Chile have so far only focused on specific faults or fault systems, and no unified and official database of active and potentially-active faults at national scale has been yet published. A regional assessment of neotectonic structures was first presented in the year 2000 including the first map of active faults and folds in Chile at 1:4,000,000 scale, as part of the World Map of Active Faults³²; maps of this database were included in review papers addressing Quaternary deformation processes in South America^{33,34} and the neotectonics of Chile³⁵. Subsequently, the South American Risk Project³⁶, promoted by the Global Earthquake Model (GEM) project, incorporated those faults into a global database³⁷. Recently, Santibañez *et al.*³⁸ produced the first map of faults in Chile³⁸ by compiling published studies including the 1:1,000,000 scale map of the Chilean Geological Survey³⁹, and discussing the relation between regional tectonics, the recent instrumental crustal earthquakes, and major long-lived fault systems (active at $>10^7$ yr timescales).

Here, we present the CHilean Database of Active Faults (CHAF), a unified database of continental faults in Chile, within the South American continental plate (Figs. 1–3), which includes all the previous studies as well as newly-identified faults, using a common mapping scale and unified geomorphic criteria. We present basic statistics of fault and fault system geometrical characteristics, and a first-order estimate of maximum earthquake magnitudes using empirical relations. Our database is a contribution to the world compilation of active faults, with implications in various aspects of earth science research including geodynamics, volcanotectonics, paleoseismology, seismotectonics, studies of future earthquakes, exploration and exploitation of geothermal resources, structural control on landslides and volcanism, landscape evolution models, and seismic hazard assessments.

Methods

Fault mapping. Remote sensing data including aerial photographs, satellite images, and more recently Digital Elevation Models (DEM) have allowed the identification of geomorphic features as well as the application of quantitative morphological analyses to map topographic attributes with applications on active tectonic and structural geology studies^{40–44}. We applied classical techniques in tectonic geomorphology summarized in seminal textbooks^{45–47} for mapping newly-identified faults and remapping structures from previous studies at a uniform 1:25,000 scale. We rely on our past experience in mapping active faults in different tectonic environments using field observations and remote sensing data^{16,48–56}, in addition to the criteria used in previous active fault databases^{57–61}. We paid special attention to interpreting fault trace continuity using a uniform mapping scale based on the surface expression of faults, not the inferred seismogenic expression at depth. The latter needs to be interpreted on the base of particular assumptions, and is therefore beyond the scope of our database. Our database is based on direct surface evidences. For mapping, we used hillshade and slope maps created using QGIS v. 3.10 (www.qgis.org) from DEMs derived from TanDEM-X data (12 m resolution) available for almost the entire region and from airborne LiDAR data (1 m, 2.5 m, and 5 m resolution) available along stretches of the Coastal Cordillera and along specific fault systems. TanDEM-X DEMs were provided by the German Aerospace Center (DLR) under Science Proposals GEOL0845, GEOL1209, GEOL1628, and GEOL0707 via the DLR science portal (<https://tandemx-science.dlr.de/>). LiDAR data was provided by Digimapas Chile and Forestal Arauco under collaboration agreements. Both datasets may be obtained from the authors on a reasonable request (see Usage Notes).

Data classification and analysis. The database described in this study contains a line vector and metadata associated with each fault. The fields included in the metadata are reported in detail in the Data Records section. Faults in the CHAF database are grouped into fault systems and classified in terms of their estimated activity.

Fault system classification. We define a fault system as the population of faults distributed in a particular region that bear similarities in strike, kinematics, length distribution, and age. Fault system names have been considered on the base of previous studies, when existing (Table 1). Fault systems may or may not have a specific fault linkage geometry. For example, faults grouped into the CCTF and EWTS systems are kinematically but not geometrically linked, whereas faults grouped into the LOFS and LOTF are geometrically and kinematically linked (Fig. 1). In general, faults strands grouped in a fault system have similar strikes (Fig. 1) and fault length distributions (Fig. 4c, d). The defined fault systems may or may not be related to a certain bedrock unit and should not be considered as tectonic provinces, which encompass larger temporal and spatial scales.

Fault traces have been assigned a *type* attribute based on four classes: (1) *blind*: faults that do not reach the surface as a break in the landscape, but may be associated with a fold or flexure; (2) *covered*: faults that are covered

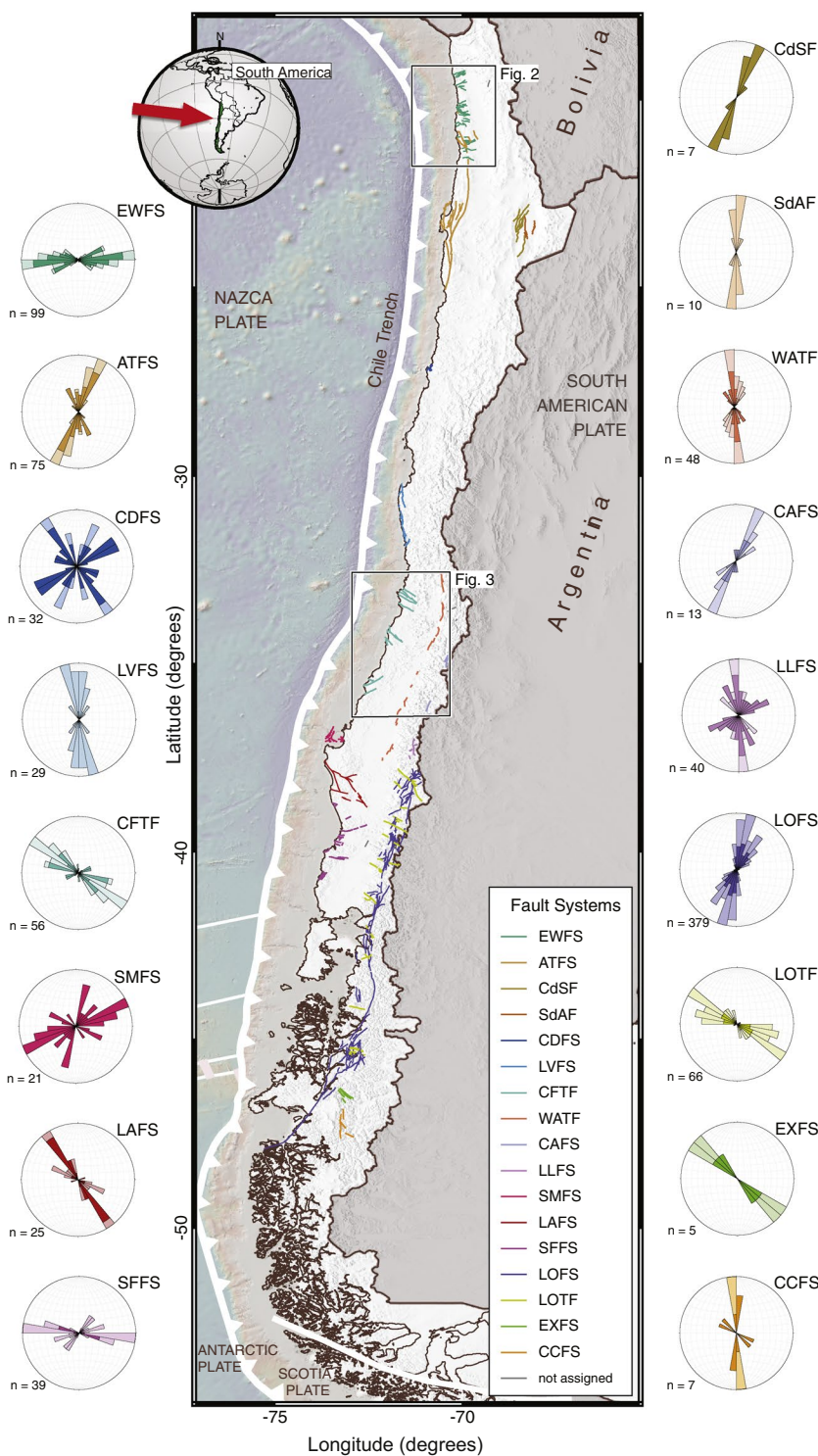


Fig. 1 The CHAF database. Map of active and potentially-active faults colour-coded by fault system and shaded-relief topography from the SRTM30_plus dataset (http://topex.ucsd.edu/WWW_html/srtm30_plus.html). See Table 1 for Fault System names and basic statistics. Rose diagrams showing strike distributions for main fault systems (n = number of fault traces). Map made using QGIS 3.10 (www.qgis.org).

by undeformed young deposits; (3) *inferred*: faults whose surface expression is not clear and only estimated; and (4) *observed*: faults that have a clear surface expression at the 1:25,000 mapping scale.

Fault activity is classified as following. Active faults and folds are grouped in two categories: (1) *Faults with proved activity (Proved faults)*, those associated with an historical earthquake or with robust published evidence of slip (either seismic or aseismic) during the Holocene; or (2) *Faults with probable activity (Probable faults)*, those that exhibit direct geologic or geomorphic evidence of surface ruptures or deformation that allow to posit activity

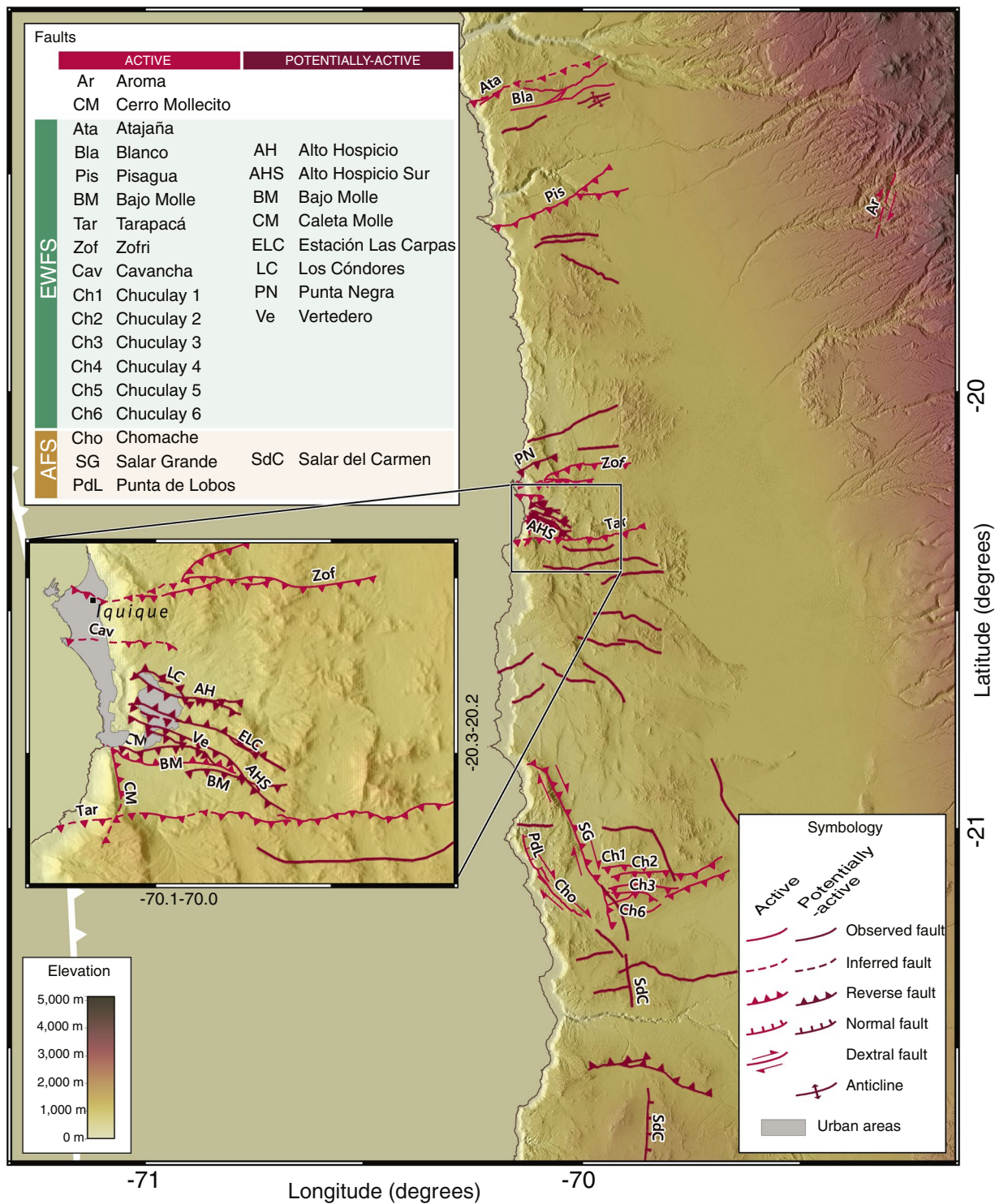


Fig. 2 Example of the CHAF database in northern Chile. Shaded-relief topography from SRTM-1 dataset (https://dds.cr.usgs.gov/srtm/version2_1/SRTM1/). Inset shows detail of reverse faults in the vicinity of the Iquique urban area. Note persistent E-W strike of these faults, grouped into the EWFS (Table 1). Map made using QGIS 3.10 (www.qgis.org).

in the past 125,000 years. The age limit for *Probably active faults* is defined by the last interglacial period (Marine Isotope Stage 5e), when a distinct marine terrace was formed along most of the Pacific coastline^{52,62}, which constitutes a suitable temporal geomorphic marker to observe fault offsets and classify fault activity. *Fault with possible activity (Possible faults)* integrate a third category, when geologic or geomorphic evidences of surface ruptures or deformation affecting the landscape allow to posit activity during the Quaternary period. For this latter case, deformed geomorphic markers include the fluvial network, pediment and alluvial surfaces, and glacial features.

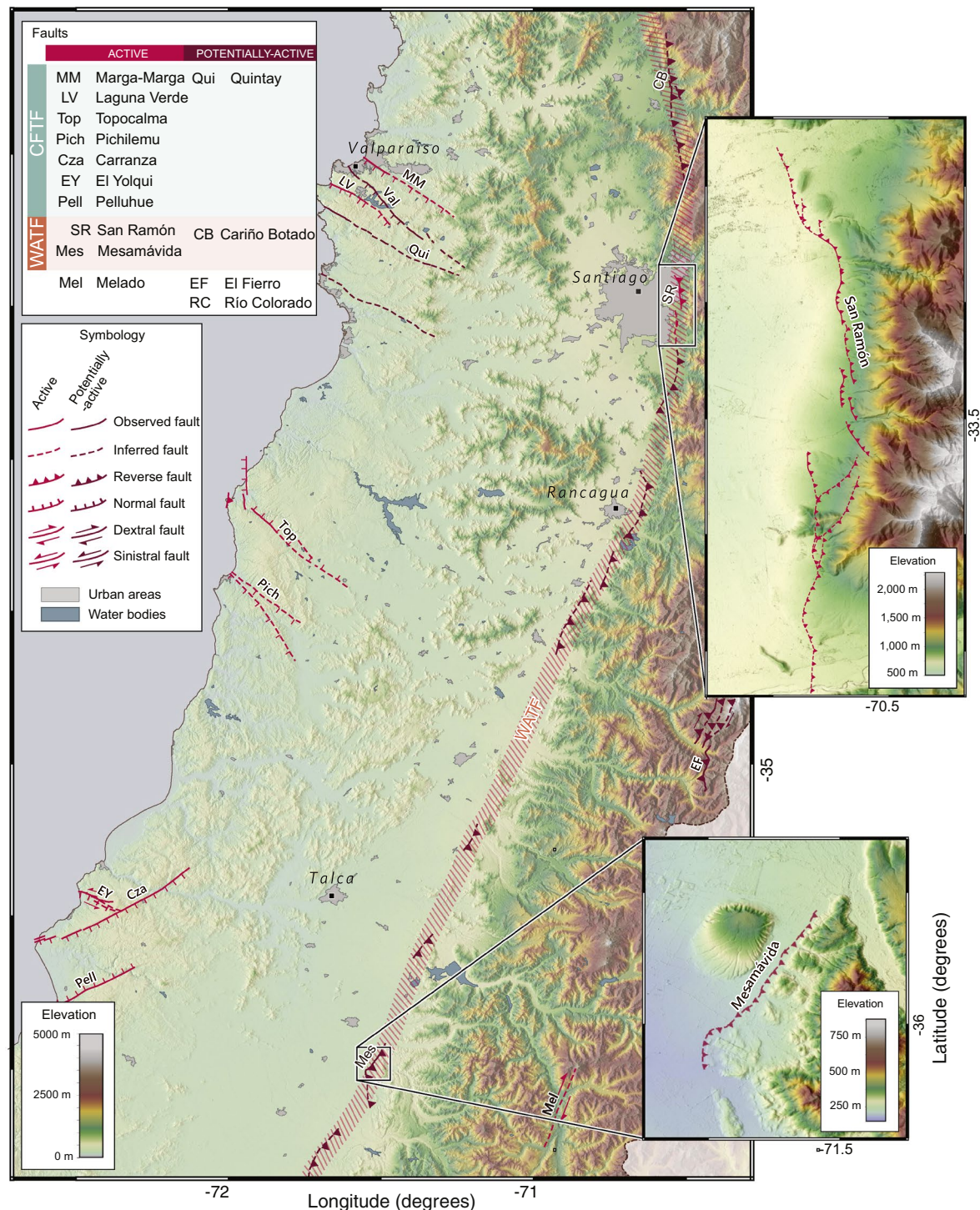


Fig. 3 Example of the CHAF database in Metropolitan and central Chile. Shaded-relief topography from SRTM-1 dataset (https://dds.cr.usgs.gov/srtm/version2_1/SRTM1/). Upper inset shows thrust faults from the San Ramón Fault, part of the Western Andean Thrust Front fault system (Table 1), adjacent to the urban region of Santiago, Chile's capital. Lower inset shows thrust faults of the Mesamávida Fault, a newly-identified structure from the same fault system. Map made using QGIS 3.10 (www.qgis.org).

Data Records

The dataset presented here is stored in the Pangaea repository⁶³, in ESRI Shapefile, Google Earth kmz, and spreadsheet xlsx formats. The dataset contains 958 records organized in 36 fields. Each record describes a single fault strand, which is part of a fault and grouped into a fault system. The 36 fields of the database may be grouped into: Identification (fields 1 to 8); Geometry (fields 9 to 19); Activity (fields 20 to 28); Historical seismicity (fields 29 to 32); Notes and references (33 to 36). The CHAF database includes 118 references^{4,27,29,31,39,48,56,64–162}.

Name	Code	No of faults	Mean strike	Number Proved faults	Number Probable faults	Number Possible faults	Fault System References*
Atacama	ATFS	75	72	29	34	12	30,168
Central Andean	CAFS	13	40	1	1	11	96
Cachet	CCFS	7	113	0	6	1	56
Caldera	CDFS	32	87	0	8	24	62
Central Coastal Forearc	CFTF	56	116	11	25	20	52,54 , This study
Cordillera de la Sal	CdSF	9	23	0	0	9	169
East-West	EWFS	99	89	2	53	44	66
Exploradores	EXFS	5	134	0	0	5	56
Lanalhue	LAFS	25	134	0	20	5	122 , This study
Lago Laja	LLFS	40	101	9	30	1	48
Liquine-Ofqui	LOFS	380	53	2	354	23	49,153
Liquine-Ofqui Transverse	LOTF	66	119	0	22	44	142,153
Los Vilos-Puerto Aldea	LVFS	29	105	0	2	27	This study
South-Central Coastal Forearc	SFFS	39	79	0	2	37	This study
Santa Maria	SMFS	21	66	1	20	0	51,123,162
Salar de Atacama	SdAF	10	74	0	10	0	107
Western Andean Thrust Front	WATF	48	97	25	1	22	31,170 , This study
	not assigned	5	29	1	1	3	

Table 1. Fault systems of the CHAF Database. *Key references of the Quaternary activity of the Fault System and definition of the fault system, for a complete reference list see the database and Supplementary File 1.

Identification.

1. **Fault trace id** (short name: F_id): Unique fault trace six-digit identifier, coded as “100101” (1/001/01: sector/fault/trace).
2. **Fault system** (short name: F_system): Mayor group of faults at regional scale.
3. **Fault name** (short name: F_name): Name of the main fault
4. **Trace name** (short name: FT_name): Name of the fault trace or segment
5. **Mapping data** (short name: map_data): Data used for fault mapping (TDX, LiDAR, Seismic reflection, microseismicity).
6. **Latitude** (short name: Lat): Latitude coordinate of the trace centre.
7. **Longitude** (short name: Lon): Longitude coordinate of the trace centre.
8. **Fault type** (short name: type): Interpreted fault (observed, inferred, covered, blind).

Geometry.

9. **Geometry class** (short name: geom): structure geometry (simple fault, segmented fault, fold).
10. **Strike** (short name: strike): Strike of the fault trace.
11. **Dip** (short name: dip): Dip of the fault trace.
12. **Dip direction** (short name: dipdir): Dip direction of the fault trace.
13. **Rake** (short name: rake): Rake of the main fault.
14. **Sense of movement** (short name: sense): Sense of movement of the main fault.
15. **Fault trace length** (short name: length_km): Along-strike length of the fault trace.
16. **Minimum depth** (short name: min_z_km): Minimum depth of the fault trace.
17. **Maximum depth** (short name: max_z_km): Maximum depth of the fault trace.
18. **Width** (short name: width_km): Down-dip width depth of the fault trace.
19. **Area** (short name: area_km²): Fault area in km².

Activity.

20. **Age of activity** (short name: age): This field includes four classes: Historic; Holocene; Late Quaternary (<125 ka); Quaternary.
21. **Activity class** (short name: activity): This field includes three classes: proved (based on paleoseismic trenching or historical activity); probable (based on geomorphic criteria and/or unequivocally aligned crustal microseismicity); possible (geomorphic criteria).
22. **Recent seismic activity** (short name: recent_act): Most-recent evidences of faulting and displacement.
23. **Faulting onset** (short name: onset): Estimated age for the onset of faulting.
24. **Throw rate** (short name: throw_rate): Vertical slip rate in mm/yr.
25. **Horizontal slip rate** (short name: h_slip_rate): Horizontal slip rate in mm/yr.
26. **Slip rate** (short name: slip_rate): Fault slip rate in mm/yr.

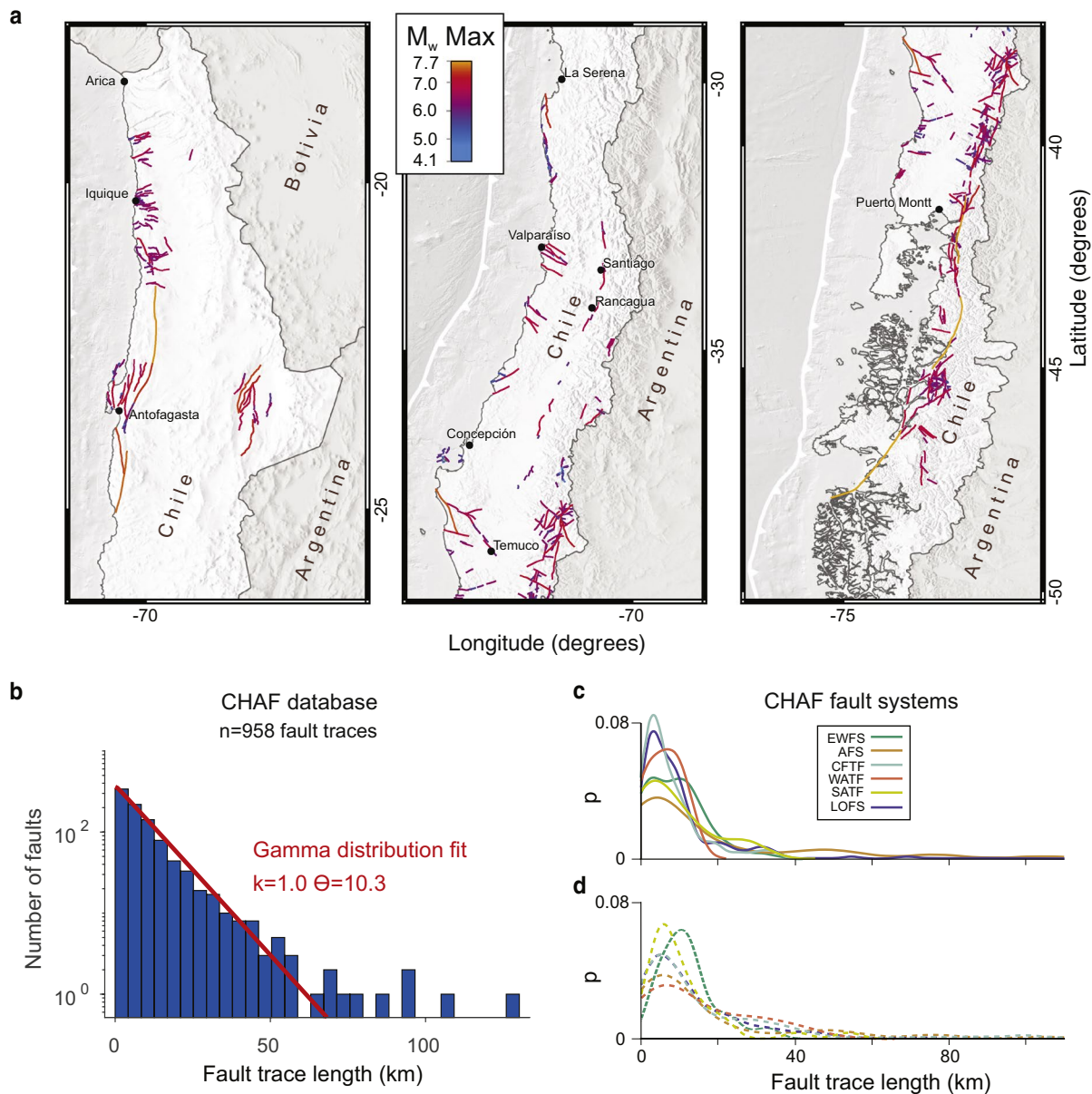


Fig. 4 CHAF database statistics. **(a)** map of faults colour-coded by maximum earthquake magnitude expected for individual fault strands estimated using empirical relations¹⁶³. Dots denote cities with more than 200,000 inhabitants. **(b)** distribution of fault lengths of the entire database. Note trade-off at ~60 km for gamma distribution fit. Faults with long traces belong to the LOFS and ATFS, both long-lived ($>10^7$ years) strike-slip systems. **(c)** probability density functions of fault length for proven and probable faults grouped by fault system (p: probability density). **(d)** same as c for possible faults. Note similarity in fault length distributions for most fault systems.

- 27. **Aseismic slip evidence** (short name: aseismic_slip): Evidences for aseismic slip from paleoseismic or geodetic data.
- 28. **Paleoseismic evidence** (short name: paleo_ev): Evidences of past earthquakes from paleoseismic data.

Historical seismicity.

- 29. **Associated seismicity** (short name: ass_seim): Related microseismicity or historical earthquakes.
- 30. **Maximum registered magnitude** (short name: Mmax_r): Maximum magnitude of an instrumentally-recorded earthquake in moment tensor magnitude scale.
- 31. **Maximum estimated magnitude** (short name: Mmax_e): Maximum magnitude of an estimated earthquake in moment tensor magnitude scale.
- 32. **Recurrence interval** (short name: rec_int): Earthquake recurrence interval of the maximum recorded or estimated magnitude.

Notes and references.

33. **Notes** (short name: notes): Notes and comments.
34. **Trace source** (short name: source): Source of the fault trace (ref: digitized from published study or studies; Unif: re-mapped based on a published study; Map: based on new geomorphic interpretations made in this study).
35. **Source mapping scale** (short name: map_scale): Scale of the source map, in case of a previously-mapped fault.
36. **References** (short name: refs): Published studies used as reference for mapping and/or metadata. A complete list of all the references used in the database is provided in the Supplementary File 1.

Statistical data analysis. We grouped fault traces of the CHAF database into 17 Fault Systems (Table 1). The comprehensive mapping scale of the database allows estimating first-order statistics of fault traces and fault systems that may be relevant and of interest to various different disciplines in Earth sciences. Empirical relations estimated from the surface rupture length and magnitude of historical earthquakes¹⁶³ provide a first-order assessment of seismic hazard implications from the CHAF database (Fig. 4a). The distribution of fault length of the entire database (Fig. 4b) suggests that faults are self-similar until a length of ~60 km. Longer traces might require higher-resolution topography and/or mapping at a detailed scale for subdivision, or might reflect mature faults that have accumulated larger magnitudes of deformation resulting in higher geometrical connectivity.

Technical Validation

The CHAF database is difficult to validate by any designed experiment. The metadata of our database follows criteria established and validated by governmental institutions of different countries (i.e., USGS¹⁶⁴, GNS^{165,166}, AIST¹⁶⁷, GEM^{57,61}, and CCAF⁶⁰). The most important validation procedure will be the occurrence of a forthcoming earthquake on a mapped and properly-classified fault. However, another validation procedure is the comparison with independently-made maps published in previous studies. All these references used in the compilation of the active fault database are included as “Codes” in the digital files, allowing to check the original publication and compare the fault traces. The complete list of references in the database is provided also separately in the Supplementary File 1. The original DEM data may be provided from the authors based on reasonable request, for any project that seeks an independent validation procedure.

We validate the grouping of individual mapped fault traces into fault systems by analysing the variation in fault strike (Fig. 1) and fault length (Fig. 4b–d). All the individual fault systems have similar length distributions, both for probable and possible faults (Fig. 4b).

The present first version of the CHAF database is intended to be the start of a long-term community-based project. To achieve this goal, we created the website www.fallasactivas.cl that includes a map server to visualize the fault traces, fault systems, and associated metadata. Satellite imagery and hillshade maps created from the DEMs used for mapping have been also included. The website contains a blog aimed at obtaining feedback from the community and to allow for the submission of relevant new data on mapped faults or newly-identified unmapped faults, to update the database.

Usage Notes

The LiDAR data used for mapping previously- and newly-identified faults was in part acquired from the company Digimapas Chile and in part donated by Forestal Arauco to the CYCLO project under a confidentiality agreement. The data may be obtained from the corresponding author based on a reasonable request and a Memorandum of Understanding (MoU); a draft MoU may be found in the Supplementary Materials. TanDEM-X DEMs may be obtained from the corresponding author based on a reasonable request and from the German Aerospace Center (DLR).

Received: 8 July 2020; Accepted: 2 December 2020;

Published online: 20 January 2021

References

1. Willis, B. & Wood, H. A Fault Map of California. *Science* **59**, 310–311 (1924).
2. Kerr, P. F. & Schenck, H. G. Active Thrust-faults in San Benito County, California. *Bulletin of the Geological Society of America* **36**, 465–494 (1925).
3. Hollingsworth, J., Ye, L. & Avouac, J. P. Dynamically triggered slip on a splay fault in the Mw 7.8, 2016 Kaikoura (New Zealand) earthquake. *Geophysical Research Letters* **44**, 3517–3525 (2017).
4. Farias, M., Comte, D., Roecker, S., Carrizo, D. & Pardo, M. Crustal extensional faulting triggered by the 2010 Chilean earthquake: The Pichilemu Seismic Sequence. *Tectonics* **30**, TC2011, <https://doi.org/10.1029/2011TC002888> (2011).
5. Quigley, M. *et al.* Surface rupture during the 2010 Mw 7.1 Darfield (Canterbury) earthquake: Implications for fault rupture dynamics and seismic-hazard analysis. *Geology* **40**, 55–58 (2012).
6. Barnhart, W. D., Hayes, G. P. & Gold, R. D. The July 2019 Ridgecrest, California, Earthquake Sequence: Kinematics of Slip and Stressing in Cross-Fault Ruptures. *Geophysical Research Letters* **46**, 11859–11867 (2019).
7. Beavan, J., Fielding, E., Motagh, M., Samsonov, S. & Donnelly, N. Fault location and slip distribution of the 22 February 2011 Mw 6.2 Christchurch, New Zealand, earthquake from geodetic data. *Seismological Research Letters* **82**, 789–799 (2011).
8. Morell, K. D. *et al.* Seismic hazard analyses from geologic and geomorphic data: Current and future challenges. *Tectonics* **39**, e2018TC005365, <https://doi.org/10.1029/2018tc005365> (2020).
9. Boncio, P., Lavecchia, G. & Pace, B. Defining a model of 3D seismogenic sources for Seismic Hazard Assessment applications: the case of central Apennines (Italy). *Journal of Seismology* **8**, 407–425 (2004).
10. Ishiyama, T., Sato, H., Abe, S., Kawasaki, S. & Kato, N. High-resolution 3D seismic reflection imaging across active faults and its impact on seismic hazard estimation in the Tokyo metropolitan area. *Tectonophysics* **689**, 79–88 (2016).

11. Field, E. H. *et al.* Uniform California earthquake rupture forecast, version 2 (UCERF 2). *Bulletin of the Seismological Society of America* **99**, 2053–2107 (2009).
12. Simpson, D. Triggered earthquakes. *Annual Review of Earth and Planetary Sciences* **14**, 21–42 (1986).
13. Cucci, L., Currenti, G., Palano, M. & Tertulliani, A. The Dewatering of the Fucino Lake Did Not Promote the M7.1 1915 Fucino Earthquake: Insights From Numerical Simulations. *Tectonics* **37**, 2633–2646, <https://doi.org/10.1029/2017tc004940> (2018).
14. González, P. J., Tiampo, K. F., Palano, M., Cannavò, F. & Fernández, J. The 2011 Lorca earthquake slip distribution controlled by groundwater crustal unloading. *Nature Geoscience* **5**, 821–825, <https://doi.org/10.1038/ngeo1610> (2012).
15. Trumpy, E. *et al.* Data integration and favourability maps for exploring geothermal systems in Sicily, southern Italy. *Geothermics* **56**, 1–16 (2015).
16. Riedl, S., Melnick, D., Mibe, G., Njue, L. & Strecker, M. R. Continental rifting at magmatic centres: structural implications from Late Quaternary Menengai Caldera, central Kenya Rift. *Journal of the Geological Society of London* **177**, 153–169 (2020).
17. Noorollahi, Y., Itoi, R., Fujii, H. & Tanaka, T. GIS model for geothermal resource exploration in Akita and Iwate prefectures, northern Japan. *Computers & geosciences* **33**, 1008–1021 (2007).
18. Chambefort, I., Buscarlet, E., Wallis, I. C., Sewell, S. & Wilmarth, M. Ngatamariki geothermal field, New Zealand: Geology, geophysics, chemistry and conceptual model. *Geothermics* **59**, 266–280 (2016).
19. Gómez-Vasconcelos, M. G. *et al.* Crustal extension in the Tongariro graben, New Zealand: Insights into volcano-tectonic interactions and active deformation in a young continental rift. *GSA Bulletin* **129**, 1085–1099 (2017).
20. Zhao, D., Santosh, M. & Yamada, A. Dissecting large earthquakes in Japan: Role of arc magma and fluids. *Island Arc* **19**, 4–16 (2010).
21. Heidbach, O. *et al.* Global crustal stress pattern based on the World Stress Map database release 2008. *Tectonophysics* **482**, 3–15 (2010).
22. Mariucci, M. T. & Montone, P. Database of Italian present-day stress indicators, IPSI 1.4. *Scientific data* **7**, 1–11 (2020).
23. Sbarra, P. *et al.* Inferring the depth of pre-instrumental earthquakes from macroseismic intensity data: a case-history from Northern Italy. *Scientific Reports* **9**, 15583, <https://doi.org/10.1038/s41598-019-51966-4> (2019).
24. Barberio, M. D. *et al.* New observations in Central Italy of groundwater responses to the worldwide seismicity. *Scientific Reports* **10**, 17850, <https://doi.org/10.1038/s41598-020-74991-0> (2020).
25. Diederichs, A. *et al.* Unusual kinematics of the Papatea fault (2016 Kaikōura earthquake) suggest anelastic rupture. *Science Advances* **5**, eaax5703 (2019).
26. Goldberg, D. E. *et al.* Complex rupture of an immature fault zone: A simultaneous kinematic model of the 2019 Ridgecrest, CA earthquakes. *Geophysical Research Letters* **47**, e2019GL086382 (2020).
27. Alvarado, P., Barrientos, S., Saez, M., Astroza, M. & Beck, S. Source study and tectonic implications of the historic 1958 Las Melosas crustal earthquake, Chile, compared to earthquake damage. *Physics of the Earth and Planetary Interiors* **175**, 26–36, <https://doi.org/10.1016/j.pepi.2008.03.015> (2009).
28. Legrand, D. *et al.* Source parameters of the M-w=6.3 Aroma crustal earthquake of July 24, 2001 (northern Chile), and its aftershock sequence. *Journal of South American Earth Sciences* **24**, 58–68, <https://doi.org/10.1016/j.jsames.2007.02.004> (2007).
29. Mora, C., Comte, D., Russo, R., Gallego, A. & Mocanu, V. Aysen seismic swarm (January 2007) in southern Chile: analysis using Joint Hypocenter Determination. *Journal of Seismology* **14**, 683–691, <https://doi.org/10.1007/s10950-010-9190-y> (2010).
30. Cortes A, J. *et al.* Paleoseismology of the Mejillones Fault, northern Chile: Insights from cosmogenic Be-10 and optically stimulated luminescence determinations. *Tectonics* **31**, <https://doi.org/10.1029/2011tc002877> (2012).
31. Vargas, G. *et al.* Probing large intraplate earthquakes at the west flank of the Andes. *Geology* **42**, 1083–1086, <https://doi.org/10.1130/g35741.1> (2014).
32. Lavenu, A. *Maps and database of Quaternary faults in Bolivia and Chile.* (USGS, 2000).
33. Costa, C. H. *et al.* An Overview of the Main Quaternary Deformation of South America. *Revista de la Asociación Geológica Argentina* **61**, 461–479 (2006).
34. Costa, C. *et al.* Hazardous faults of South America; compilation and overview. *Journal of South American Earth Sciences* **104**, 102837, <https://doi.org/10.1016/j.jsames.2020.102837> (2020).
35. Cembrano, J. *et al.* In *The geology of Chile* (eds T. Moreno & W. Gibbons) 231–261 (The Geological Society, 2007).
36. SARA. *Research Topic 2 (RT2): Building a harmonised database of 'hazardous' crustal faults*, https://sara.openquake.org/hazard_rt2 (2016).
37. GEM. *Global Earthquake Model*, <https://blogs.openquake.org/hazard/global-active-fault-viewer> (2020).
38. Santibáñez, I. *et al.* Fallas corticales en los Andes chilenos: limitaciones geológicas y potencial sísmico. *Andean geology* **46**, 32–65 (2019).
39. Sernageomin. Mapa Geológico de Chile escala 1:1.000.000 versión digital. Servicio Nacional de Geología y Minería, Publicación Geológica Digital, No. 4 (Santiago, 2003).
40. DeLong, S. B., Hilley, G. E., Rymer, M. J. & Prentice, C. Fault zone structure from topography: Signatures of en echelon fault slip at Mustang Ridge on the San Andreas fault, Monterey County, California. *Tectonics* **29**, TC5003 (2010).
41. Ganas, A., Pavlides, S. & Karastathis, V. DEM-based morphometry of range-front escarpments in Attica, central Greece, and its relation to fault slip rates. *Geomorphology* **65**, 301–319 (2005).
42. Jordán, G., Meijninger, B., Van Hinsbergen, D., Meulenkamp, J. & Van Dijk, P. Extraction of morphotectonic features from DEMs: Development and applications for study areas in Hungary and NW Greece. *International journal of applied earth observation and geoinformation* **7**, 163–182 (2005).
43. Chorowicz, J., Dhont, D. & Gündoğdu, N. Neotectonics in the eastern North Anatolian fault region (Turkey) advocates crustal extension: mapping from SAR ERS imagery and Digital Elevation Model. *Journal of Structural Geology* **21**, 511–532 (1999).
44. Arrowsmith, J. R. & Zielke, O. Tectonic geomorphology of the San Andreas fault zone from high resolution topography: An example from the Cholame segment. *Geomorphology* **113**, 70–81 (2009).
45. Burbank, D. W. & Anderson, R. S. *Tectonic geomorphology*. (John Wiley & Sons, 2011).
46. Keller, E. A. & Pinter, N. *Active tectonics*. Vol. 19 (Prentice Hall Upper Saddle River, NJ, 1996).
47. Bull, W. B. *Tectonic geomorphology of mountains: a new approach to paleoseismology*. (John Wiley & Sons, 2008).
48. Melnick, D., Charlet, F., Echtler, H. P. & De Batist, M. Incipient axial collapse of the Main Cordillera and strain partitioning gradient between the central and Patagonian Andes, Lago Laja, Chile. *Tectonics* **25**, TC5004 (2006).
49. Melnick, D., Folguera, A. & Ramos, V. A. Structural control on arc volcanism: The Caviahue-Copahue complex, Central to Patagonian Andes transition (38°S). *Journal of South American Earth Sciences* **22**, 66–88, <https://doi.org/10.1016/j.jsames.2006.08.008> (2006).
50. Melnick, D. *et al.* Steady rifting in northern Kenya inferred from deformed Holocene lake shorelines of the Suguta and Turkana basins. *Earth and Planetary Science Letters* **331–332**, 335–346 (2012).
51. Melnick, D., Moreno, M., Motagh, M., Cisternas, M. & Wesson, R. L. Splay fault slip during the M w 8.8 2010 Maule Chile earthquake. *Geology* **40**, 251–254 (2012).
52. Jara-Muñoz, J., Melnick, D., Brill, D. & Strecker, M. R. Segmentation of the 2010 Maule Chile earthquake rupture from a joint analysis of uplifted marine terraces and seismic-cycle deformation patterns. *Quaternary Science Reviews* **113**, 171–192, <https://doi.org/10.1016/j.quascirev.2015.01.005> (2015).

53. Melnick, D. *et al.* Slip along the Sultanhanı Fault in Central Anatolia from deformed Pleistocene shorelines of palaeo-lake Konya and implications for seismic hazards in low strain regions. *Geophysical Journal International* **209**, 1431–1454 (2017).
54. Melnick, D. *et al.* Hidden Holocene Slip Along the Coastal El Yolki Fault in Central Chile and Its Possible Link With Megathrust Earthquakes. *Journal of Geophysical Research: Solid Earth* **124**, 7280–7302, <https://doi.org/10.1029/2018jb017188> (2019).
55. Yıldırım, C., Schildgen, T. F., Echler, H., Melnick, D. & Strecker, M. R. Late Neogene and active orogenic uplift in the Central Pontides associated with the North Anatolian Fault: Implications for the northern margin of the Central Anatolian Plateau, Turkey. *Tectonics* **30**, TC5005 (2011).
56. Georgieva, V. *et al.* Tectonic control on rock uplift, exhumation, and topography above an oceanic ridge collision: Southern Patagonian Andes (47°S), Chile. *Tectonics* **35**, 1317–1341, <https://doi.org/10.1002/2016TC004120> (2016).
57. Veloza, G., Styron, R., Taylor, M. & Mora, A. Open-source archive of active faults for northwest South America. *Gsa Today* **22**, 4–10 (2012).
58. Christoffersen, A. *et al.* Development of the Global Earthquake Model's neotectonic fault database. *Natural Hazards* **79**, 111–135 (2015).
59. Styron, R., Taylor, M. & Okoronkwo, K. Database of active structures from the Indo-Asian collision. *Eos, Transactions American Geophysical Union* **91**, 181–182 (2010).
60. Styron, R., García-Peláez, J. & Pagani, M. CCAF-DB: the Caribbean and Central American active fault database. *Natural Hazards & Earth System Sciences* **20** (2020).
61. Styron, R. & Pagani, M. The GEM Global Active Faults Database. *Earthquake Spectra* **36**, 160–180, <https://doi.org/10.1177/8755293020944182> (2020).
62. Marquardt, C., Lavenu, A., Ortílieb, L., Godoy, E. & Comte, D. Coastal neotectonics in Southern Central Andes: uplift and deformation of marine terraces in Northern Chile (27°S). *Tectonophysics* **394**, 193–219, <https://doi.org/10.1016/j.tecto.2004.07.059> (2004).
63. Melnick, D., Maldonado, V. & Contreras, M. Database of active and potentially-active continental faults in Chile at 1:25,000 scale. PANGAEA <https://doi.org/10.1594/PANGAEA.922241> (2020).
64. Aguilera, F. *et al.* Evaluación de los recursos geotérmicos de la Región de Los Lagos. IR-14-57, Sernageomin. (2014).
65. Allmendinger, R. W. & González, G. Invited review paper: Neogene to Quaternary tectonics of the coastal Cordillera, northern Chile. *Tectonophysics* **495**, 93–110, <https://doi.org/10.1016/j.tecto.2009.04.019> (2009).
66. Allmendinger, R. W., González, G., Yu, J., Hoke, G. & Isacks, B. Trench-parallel shortening in the Northern Chilean Forearc: Tectonic and climatic implications. *Geological Society of America Bulletin* **117**, 89–104 (2005).
67. Álvarez, L. Geología del área Valparaíso-Viña del Mar. *Instituto de Investigaciones Geológicas, Santiago, Chile*, 1–58 (1964).
68. Arancibia, G., Cembrano, J. & Lavenu, A. Transpresión dextral y partición de la deformación en la Zona de Falla Liquiñe-Ofqui, Aisén, Chile (44–45°S). *Revista Geológica De Chile* **26**, 3–22 (1999).
69. Armijo, R. *et al.* The West Andean Thrust, the San Ramón Fault, and the seismic hazard for Santiago, Chile. *Tectonics* **29**, TC2007, <https://doi.org/10.1029/2010TC002692> (2010).
70. Armijo, R. & Thiele, R. Active faulting in northern Chile: ramp stacking and lateral decoupling along a subduction plate boundary? *Earth and Planetary Science Letters* **98**, 40–61, [https://doi.org/10.1016/0012-821X\(90\)90087-E](https://doi.org/10.1016/0012-821X(90)90087-E) (1990).
71. Aron, F., Allmendinger, R. W., Cembrano, J., González, G. & Yáñez, G. Permanent fore-arc extension and seismic segmentation: Insights from the 2010 Maule earthquake, Chile. *Journal of Geophysical Research: Solid Earth* **118**, 724–739, <https://doi.org/10.1029/2012JB009339> (2013).
72. Aron, F., Cembrano, J., Astudillo, F., Allmendinger, R. W. & Arancibia, G. Constructing forearc architecture over megathrust seismic cycles: Geological snapshots from the Maule earthquake region. *Chile. Bulletin of the Geological Society of America* **127**, 464–479, <https://doi.org/10.1130/B31125.1> (2014).
73. Astudillo, L., Jara-muñoz, J., Melnick, D. & Cortés-Aranda, J. Fast Holocene slip and localized strain along the Liquiñe-Ofqui strike-slip fault system. In *International INQUA Meeting on Paleoseismology, Active Tectonics and Archeoseismology* (2018).
74. Avilés, J., Vargas, G. & Ortega, C. Estratigrafía sísmica y evidencias submarinas de tectónica activa en la falla Puerto Aldea, Tongoy, IV Región de Coquimbo, Chile. In *XIV Congreso Geológico Chileno*. (2015).
75. Barrientos, S. E. & Acevedo-Aránguiz, P. S. Seismological aspects of the 1988–1989 Lonquimay (Chile) volcanic eruption. *Journal of Volcanology and Geothermal Research* **53**, 73–87, [https://doi.org/10.1016/0377-0273\(92\)90075-O](https://doi.org/10.1016/0377-0273(92)90075-O) (1992).
76. Bucci, F., Lara, L. E. & Gutiérrez, F. The Carrán-Los Venados volcanic field and its relationship with coeval and nearby polygenetic volcanism in an intra-arc setting. *Journal of Volcanology and Geothermal Research* **308**, 70–81, <https://doi.org/10.1016/j.jvolgeores.2015.10.013> (2015).
77. Campos, A. *et al.* Área de Futrono-Lago Ranco, Región de los Lagos. Servicio Nacional de Geología y Minería. (1998).
78. Cardona, C. *et al.* Crustal seismicity associated to rapid surface uplift at Laguna del Maule Volcanic Complex, Southern Volcanic Zone of the Andes. *Journal of Volcanology and Geothermal Research* **353**, 83–94, <https://doi.org/10.1016/j.jvolgeores.2018.01.009> (2018).
79. Carrasco, S., Ruiz, J. A., Contreras-Reyes, E. & Ortega-Culaciati, F. Shallow intraplate seismicity related to the Illapel 2015 Mw 8.4 earthquake: Implications from the seismic source. *Tectonophysics* **766**, 205–218, <https://doi.org/10.1016/j.tecto.2019.06.011> (2019).
80. Carrizo, D., González, G. & Dunai, T. Constricción neógena en la Cordillera de la Costa, norte de Chile: neotectónica y datación de superficies con 21Ne cosmogónico. *Revista geológica de Chile* **35**, 01–38, <https://doi.org/10.4067/S0716-02082008000100001> (2008).
81. Cembrano, J., Hervé, F. & Lavenu, A. The Liquiñe Ofqui fault zone: a long-lived intra-arc fault system in southern Chile. *Tectonophysics* **259**, 55–66, [https://doi.org/10.1016/0040-1951\(95\)00066-6](https://doi.org/10.1016/0040-1951(95)00066-6) (1996).
82. Cembrano, J. & Lara, L. The link between volcanism and tectonics in the southern volcanic zone of the Chilean Andes: A review. *Tectonophysics* **471**, 96–113, <https://doi.org/10.1016/j.tecto.2009.02.038> (2009).
83. Cembrano, J., Schermer, E., Lavenu, A. & Sanhueza, A. Contrasting nature of deformation along an intra-arc shear zone, the Liquiñe-Ofqui fault zone, southern Chilean Andes. *Tectonophysics* **319**, 129–149, [https://doi.org/10.1016/S0040-1951\(99\)00321-2](https://doi.org/10.1016/S0040-1951(99)00321-2) (2000).
84. Charrier, R., Farías, M., Comte, D. & Pardo, M. Active Tectonic in the Southern Central Andes, a Recent Example: the 28 August, 2004 Shallow Mw = 6.5 Earthquake. In *AGU fall meeting*. (2014).
85. Comte, D., Farias, M., Roecker, S. & Russo, R. The nature of the subduction wedge in an erosive margin: Insights from the analysis of aftershocks of the 2015 Mw 8.3 Illapel earthquake beneath the Chilean Coastal Range. *Earth and Planetary Science Letters* **520**, 50–62, <https://doi.org/10.1016/j.epsl.2019.05.033> (2019).
86. Cortés, A. J. *et al.* Paleoseismology of the Mejillones Fault, northern Chile: Insights from cosmogenic 10 Be and optically stimulated luminescence determinations. *Tectonics* **31**, TC2017, <https://doi.org/10.1029/2011TC002877> (2012).
87. Cortés-Aranda, J. *Activité des failles de la plaque supérieure dans l'avant-arc côtier du nord du Chili (~23°30'S): Paléosismologie, implications néotectoniques et relation avec le cycle de subduction*. PhD thesis, Université Toulouse III - Paul Sabatier, (2012).
88. Cortés-Aranda, J., González, G., Rémy, D. & Martinod, J. Normal upper plate fault reactivation in northern Chile and the subduction earthquake cycle: From geological observations and static Coulomb Failure Stress (CFS) change. *Tectonophysics* **639**, 118–131, <https://doi.org/10.1016/j.tecto.2014.11.019> (2015).
89. David, C. *Comportement actuel de l'avant-arc et de l'arc du coude de Arica dans l'orogénèse des Andes Centrales*. PhD thesis, Université Toulouse III - Paul Sabatier, (2007).

90. Duhart, P. *et al.* Geología del área Los Lagos-Malalhue, Región de los Lagos. Servicio Nacional de Geología y Minería. Serie Geología Básica (81). (Sernageomin, 2003).
91. Ewiak, O., Victor, P. & Onccken, O. Investigating multiple fault rupture at the Salar del Carmen segment of the Atacama Fault System (northern Chile): Fault scarp morphology and knickpoint analysis. *Tectonics* **34**, 187–212, <https://doi.org/10.1002/2014TC003599> (2015).
92. Forsythe, R. & Nelson, E. Geological manifestations of ridge collision: Evidence from the Golfo de Penas-Taitao basin, Southern Chile. *Tectonics* **4**, 477–495 (1985).
93. Gana, P., Wall, R. & Gutiérrez, A. Mapa geológico del área de Valparaíso-Curacaví, regiones de Valparaíso y Metropolitana. Servicio Nacional de Geología y Minería. (1996).
94. García, M. & Fuentes, G. Carta Cuya, Regiones de Arica y Parinacota y de Tarapacá. Servicio Nacional de Geología y Minería. Carta Geológica de Chile. Serie Geología Básica (146) (2012).
95. García-Pérez, T. *et al.* Insights on the structural control of a Neogene forearc basin in Northern Chile: A geophysical approach. *Tectonophysics* **736**, 1–14, <https://doi.org/10.1016/j.tecto.2018.04.003> (2018).
96. Giambiagi, L. *et al.* Geomechanical model for a seismically active geothermal field: Insights from the Tinguiririca volcanic-hydrothermal system. *Geoscience Frontiers* **10**, 2117–2133 (2019).
97. Glodny, J. *et al.* Differential Late Paleozoic active margin evolution in South-Central Chile (37°S–40°S) – the Lanalhue Fault Zone. *Journal of South American Earth Sciences* **26**, 397–411, <https://doi.org/10.1016/j.jsames.2008.06.001> (2008).
98. González, A. *Análisis estructural entre los valles del Río Tinguiririca y Teno, Cordillera Principal de Chile Central: Microsismicidad y Geología Superficial*. Bachelor thesis, Universidad de Chile, (2008).
99. González, G. & Carrizo, D. Segmentación, cinemática y cronología relativa de la deformación tardía de la Falla Salar del Carmen, Sistema de Fallas de Atacama, (23°40'S), norte de Chile. *Revista geológica de Chile* **30**, 223–244, <https://doi.org/10.4067/S0716-02082003000200005> (2003).
100. González, G., Cembrano, J., Carrizo, D., Macci, A. & Schneider, H. The link between forearc tectonics and Pliocene–Quaternary deformation of the Coastal Cordillera, northern Chile. *Journal of South American Earth Sciences* **16**, 321–342, [https://doi.org/10.1016/S0895-9811\(03\)00100-7](https://doi.org/10.1016/S0895-9811(03)00100-7) (2003).
101. González, G. *et al.* Upper plate reverse fault reactivation and the unclamping of the megathrust during the 2014 northern Chile earthquake sequence. *Geology* **43**, 671–674, <https://doi.org/10.1130/G36703.1> (2015).
102. González-Alfaro, J. *et al.* Abrupt increase in the coastal uplift and earthquake rate since ~40 ka at the northern Chile seismic gap in the Central Andes. *Earth and Planetary Science Letters* **502**, 32–45, <https://doi.org/10.1016/j.epsl.2018.08.043> (2018).
103. Guzmán-Marín, P., Lira, M. P., Tassara, A. & Urrutia, R. Nuevos antecedentes tectónicos del Sistema de Fallas Liquiñe-Ofqui en la Cuenca de Intra-arco del Lago Maihue (40° 16' S 72° W), Andes del Sur, Chile. In *XIV Congreso Geológico Chileno*. (2015).
104. Haberland, C., Rietbrock, A., Lange, D., Bataille, K. & Hofmann, S. Interaction between forearc and oceanic plate at the south-central Chilean margin as seen in local seismic data. *Geophysical Research Letters* **33**, L23302–L23302, <https://doi.org/10.1029/2006GL028189> (2006).
105. Heinze, B. *Active Intraplate Faulting in the Forearc of North Central Chile*. PhD thesis, Free University of Berlin, (2003).
106. Hervé, F. *et al.* Ultramafic rocks in the North Patagonian Andes: Is their emplacement associated with the Neogene tectonics of the Liquiñe-Ofqui Fault Zone? *Andean Geology* **44**, 1–1, <https://doi.org/10.5027/andgeoV44n1-a01> (2017).
107. Jordan, T. E. *et al.* Active faulting and folding without topographic expression in an evaporite basin, Chile. *Geological Society of America Bulletin* **114**, 1406–1421, 10.1130/0016-7606(2002)114<1406:AFAFWT>2.0.CO;2 (2002).
108. Lange, D. *et al.* First seismic record for intra-arc strike-slip tectonics along the Liquiñe-Ofqui fault zone at the obliquely convergent plate margin of the southern Andes. *Tectonophysics* **455**, 14–24, <https://doi.org/10.1016/j.tecto.2008.04.014> (2008).
109. Lara, L. & Moreno, H. Geología del área Liquiñe—Neltume. Servicio Nacional de Geología y Minería. Serie Geología Básica **832**, 23 (2004).
110. Lara, L. E., Cembrano, J. & Lavenu, A. La Zona de Falla Liquiñe-Ofqui: Antecedentes de su evolución cuaternaria e implicancias para el volcanismo activo en los Andes del Sur. In *X Congreso Geológico Chileno*. (2006).
111. Lara, L. E., Cembrano, J. & Lavenu, A. Quaternary Vertical Displacement along the Liquiñe-Ofqui Fault Zone: Differential Uplift and Coeval Volcanism in the Southern Andes? *International Geology Review* **50**, 975–993, <https://doi.org/10.2747/0020-6814.50.11.975> (2008).
112. Lara, L. E., Lavenu, A., Cembrano, J. & Rodríguez, C. Structural controls of volcanism in transversal chains: Resheared faults and neotectonics in the Cordón Caulle-Puyehue area (40.5°S), Southern Andes. *Journal of Volcanology and Geothermal Research* **158**, 70–86, <https://doi.org/10.1016/j.jvolgeores.2006.04.017> (2006).
113. Lara, L. E. & Moreno, H. Geología del Complejo Volcánico Puyehue-Cordón Caulle. Región de Los Lagos, Chile. Carta geológica de Chile. Serie Geología Básica (99). (2006).
114. Lara, L. E. & Moreno, H. Geología del Complejo Volcánico Antillanca, Región de los Lagos. Servicio Nacional de Geología y Minería. Carta Geológica de Chile. Serie Geología Básica, 1 mapa escala 1, 50.000 (2012).
115. Lavenu, A. Fallas Cuaternarias de Chile. Servicio Nacional de Geología y Minería (SERNAGEOMIN). *Boletín* **62**(71 p), 70–70 (2005).
116. Lavenu, A. & Cembrano, J. Deformación compresiva cuaternaria en la Cordillera Principal de Chile central (Cajón del Maipo, este de Santiago). *Revista geológica de Chile* **35**, 233–252, <https://doi.org/10.4067/S0716-02082008000200003> (2008).
117. Legrand, D., Barrientos, S., Bataille, K., Cembrano, J. & Pavez, A. The fluid-driven tectonic swarm of Aysen Fjord, Chile (2007) associated with two earthquakes ($M_w=6.1$ and $M_w=6.2$) within the Liquiñe-Ofqui Fault Zone. *Continental Shelf Research* **31**, 154–161, <https://doi.org/10.1016/j.csr.2010.05.008> (2011).
118. Lemus H. M. *et al.* Evaluación de los recursos geotérmicos de la región de los ríos. IR-15-59. Sernageomin., (2015).
119. Marquardt, C. *Neotectónica de la franja costera y aportes a la geología regional entre Caldera y Caleta Pajonal (27°00'–27°45'), III Región de Atacama*. Bachelor thesis, Universidad de Chile, (1999).
120. Medina, J. *Caracterización de la falla Cariño Botado (32°30'S) y su relación al West Andean Thrust System (WATS)*. Bachelor thesis, Universidad de Chile, (2018).
121. Mella, M. *et al.* Geología del Área Valdivia-Corral, Región de Los Ríos. Servicio Nacional de Geología y Minería. Carta Geológica de Chile. Serie Geología Básica (137). (2012).
122. Melnick, D., Bookhagen, B., Strecker, M. S. & Echtler, H. P. Segmentation of megathrust rupture zones from fore arc deformation patterns over hundreds to millions of years, Arauco peninsula, Chile. *Journal of Geophysical Research* **114**, B01407 (2009).
123. Melnick, D., Bookhagen, B., Echtler, H. P. & Strecker, M. R. Coastal deformation and great subduction earthquakes, Isla Santa María, Chile (37°S). *Bulletin of the Geological Society of America* **118**, 1463–1480 (2006).
124. Moreno, H. & Lara, L. Geología del complejo volcánico Mocho-Choshuenco, Región de Los Ríos. Servicio Nacional de Geología y Minería. Carta Geológica de Chile. Serie Geología Básica (107). (2007).
125. Moreno, H. & Lara, L. Geología del Área Pucón–Curarrehue, Regiones de La Araucanía y de los Ríos: Santiago, Chile, Servicio Nacional de Geología y Minería. Carta Geológica de Chile, Serie Geología Básica, 1 mapa, escala 1:100,000. (2008).
126. Muñoz, B. & Stern, J. C. R. The quaternary volcanic belt of the southern continental margin of South America: Transverse structural and petrochemical variations across the segment between 38°S and 39°S. *Journal of South American Earth Sciences* **1**, 147–161, [https://doi.org/10.1016/0895-9811\(88\)90032-6](https://doi.org/10.1016/0895-9811(88)90032-6) (1988).

127. Muñoz, E., Sepulveda, S. & Rebolledo, S. Nuevos antecedentes sobre la falla Marga-Marga y sus implicancias en el peligro sísmico. In *XIII Congreso Geológico Chileno*. (2012).
128. Naranjo, J. A. Interpretación de la actividad cenozoica superior a lo largo de la Zona de Falla Atacama, Norte de Chile. *Andean Geology* **31**, 43–55, <https://doi.org/10.5027/andgeov14n2-a06> (1987).
129. Naranjo, J. A. & Moreno, H. Geología del Volcán Llaima, Región de La Araucanía. Sernageomin. Escala: 1:50.000. (2005).
130. Niemeyer, H. La Megafalla Tucúcaro en el extremo sur del Salar de Atacama: una antigua zona de cizalle reactivada en el Cenozoico. *Comunicaciones* **34**, 37–45 (1984).
131. Ota, Y., Miyazaki, T., Paskoff, R. & Koba, M. Plio-Quaternary marine terraces and their deformation along the Altos de Talinay, North-Central Chile. *Andean Geology* **22**, 89–102, <https://doi.org/10.5027/ANDGEOV22N1-A05> (1995).
132. Pérez, P., Riquelme, R. & Cembrano, J. Contribución de la tectónica en el modelado del paisaje glacial Holoceno en la zona de falla Liquiñe-Ofqui, Fiordo Puyuhuapi (44°S). In *XII Congreso Geológico Chileno*. (2009).
133. Pérez-Flores, P. *et al.* Tectonics, magmatism and paleo-fluid distribution in a strike-slip setting: Insights from the northern termination of the Liquiñe-Ofqui fault System, Chile. *Tectonophysics* **680**, 192–210, <https://doi.org/10.1016/j.tecto.2016.05.016> (2016).
134. Pérez-Flores, P. *et al.* Fracture network, fluid pathways and paleostress at the Tolhuaca geothermal field. *Journal of Structural Geology* **96**, 134–148, <https://doi.org/10.1016/j.jsg.2017.01.009> (2017).
135. Pérez-Flores, P. *et al.* The effect of offset on fracture permeability of rocks from the Southern Andes Volcanic Zone, Chile. *Journal of Structural Geology* **104**, 142–158, <https://doi.org/10.1016/j.jsg.2017.09.015> (2017).
136. Piquer Romo, J. M., Yáñez, G., Rivera, O. & Cooke, D. Long-lived crustal damage zones associated with fault intersections in the high Andes of Central Chile. *Andean Geology* **46**, 223–223, <https://doi.org/10.5027/andgeoV46n2-3106> (2019).
137. Rauld, R. *Deformación cortical y peligro sísmico asociado a la falla San Ramón en el frente cordillerano de Santiago, Chile Central* (33°S). PhD thesis, Universidad de Chile, (2011).
138. Reijss, J. & McClay, K. Salar Grande pull-apart basin, Atacama Fault System, northern Chile. *Geological Society, London, Special Publications* **135**, 127–141, <https://doi.org/10.1144/GSL.SP.1998.135.01.09> (1998).
139. Reutter, K.-J. *et al.* In *The Andes* 303–325 (Springer, 2006).
140. Riesner, M. *et al.* Kinematics of the active West Andean fold-and-thrust belt (central Chile): Structure and long-term shortening rate. *Tectonics* **36**, 287–303, <https://doi.org/10.1002/2016TC004269> (2017).
141. Rosenau, M. *Tectonics of the Southern Andean intra-arc zone (38°–42°S)*. PhD thesis, Free University of Berlin, (2004).
142. Rosenau, M., Melnick, D. & Echtler, H. Kinematic constraints on intra-arc shear and strain partitioning in the southern Andes between 38°S and 42°S latitude. *Tectonics* **25**, TC4013 (2006).
143. Ruiz, S. *et al.* Intense foreshocks and a slow slip event preceded the 2014 Iquique Mw8.1 earthquake. *Science* **1165**, 1165–1169, <https://doi.org/10.1126/science.1256074> (2014).
144. Ryder, I. *et al.* Large extensional aftershocks in the continental forearc triggered by the 2010 Maule earthquake, Chile. *Geophysical Journal International* **188**, 879–890, <https://doi.org/10.1111/j.1365-246X.2011.05321.x> (2012).
145. Saillard, M. *et al.* Non-steady long-term uplift rates and Pleistocene marine terrace development along the Andean margin of Chile (31°S) inferred from 10Be dating. *Earth and Planetary Science Letters* **277**, 50–63, <https://doi.org/10.1016/j.epsl.2008.09.039> (2009).
146. Sánchez, P., Pérez-Flores, P., Arancibia, G., Cembrano, J. & Reich, M. Crustal deformation effects on the chemical evolution of geothermal systems: the intra-arc Liquiñe–Ofqui fault system, Southern Andes. *International Geology Review* **55**, 1384–1400, <https://doi.org/10.1080/00206814.2013.75731> (2013).
147. Santibáñez, I. *et al.* Evidencias Geofísicas de Actividad Neotectónica en la Falla Aeropuerto. In *XIV Congreso Geológico Chileno*. (2015).
148. Sepúlveda, N. & Quezada, J. Evidencias de deformación cuaternaria a partir del análisis morfológico de escarpes, ciudades de Iquique y Alto Hospicio. In *XIV Congreso Geológico Chileno*. (2015).
149. Sepulveda, S. A. *et al.* New Findings on the 1958 Las Melosas Earthquake Sequence, Central Chile: Implications for Seismic Hazard Related to Shallow Crustal Earthquakes in Subduction Zones. *Journal of Earthquake Engineering* **12**, 432–455, <https://doi.org/10.1080/13632460701512951> (2008).
150. Sepúlveda, T. *Neotectónica y paleoisismología de la falla Mesamávida: Evidencia de actividad cuaternaria tardía del cabalgamiento Andino Occidental (WATF) en la Región del Maule, Chile Central (36°S)*. Bachelor thesis, Universidad de Concepción, (2019).
151. Sernageomin. Geología para el Ordenamiento Territorial y la Gestión Ambiental en el área de Iquique – Alto Hospicio, Región de Tarapacá. IR-1353. (2013).
152. Sielfeld, G., Cembrano, J. & Lara, L. Transtension driving volcano-edifice anatomy: Insights from Andean transverse-to-the-orogen tectonic domains. *Quaternary International* **438**, 33–49, <https://doi.org/10.1016/j.quaint.2016.01.002> (2017).
153. Sielfeld, G., Lange, D. & Cembrano, J. Intra-arc crustal seismicity: Seismotectonic implications for the southern Andes volcanic zone, Chile. *Tectonics* **38**, 552–578 (2019).
154. Stefer, S. *et al.* Forearc uplift rates deduced from sediment cores of two coastal lakes in south-central Chile. *Tectonophysics* **495**, 129–143, <https://doi.org/10.1016/j.tecto.2009.05.006> (2010).
155. Troncoso, M., Pinto, L. & Vargas, G. Evidencia de neotectónica de la Falla Cariño Botado sobre la Zona de Falla Pocuro en la Provincia de Los Andes. In *XIV Congreso Geológico Chileno*. (2015).
156. Valdivia, D., del Valle, F., Marquardt, C. & Elgueta, S. Seismic influence in the Quaternary uplift of the Central Chile coastal margin, preliminary results. In *AGU Fall Meeting*. (2017).
157. Vargas Easton, G. *et al.* Submarine earthquake rupture, active faulting and volcanism along the major Liquiñe–Ofqui Fault Zone and implications for seismic hazard assessment in the Patagonian Andes. *Andean Geology* **40**, 141–171, <https://doi.org/10.5027/andgeoV40n1-a07> (2013).
158. Villalobos Claramunt, A. A. *Fallas Mititus y Naguayán: evaluación del potencial sismogénico mediante análisis geomorfológico*. Bachelor thesis, Universidad Católica del Norte, (2014).
159. Villalobos-claramunt, A., Vargas, G. & Maksymowicz, A. Evidencias paleoisismológicas del origen cortical de la Crisis Sísmica del año 2007 en la región de Aysén. In *XIV Congreso Geológico Chileno*. (2015).
160. Wall, R., Gana, P. & Gutiérrez, A. Mapa geológico del área de San Antonio-Melipilla: Regiones de Valparaíso, Metropolitana y del Libertador General Bernardo O'Higgins. Sernageomin. (1996).
161. Wicks, C., de la Llera, J. C., Lara, L. E. & Lowenstern, J. The role of dyking and fault control in the rapid onset of eruption at Chaitén volcano, Chile. *Nature* **478**, 374–377, <https://doi.org/10.1038/nature10541> (2011).
162. Jara-Muñoz, J. *et al.* Quantifying offshore forearc deformation and splay-fault slip using Pleistocene drowned shorelines, Arauco Bay, Chile. *J. Geophys. Res.* **122**, 4529–4558 (2017).
163. Wells, D. L. & Coppersmith, K. J. New empirical relationships among magnitude, rupture length, rupture width, rupture area, and surface displacement. *Bulletin of the seismological Society of America* **84**, 974–1002 (1994).
164. USGS. *Quaternary Fault and Fold Database for the Nation*, <https://pubs.usgs.gov/fs/2004/3033/fs-2004-3033.html> (2004).
165. Langridge, R. *et al.* The New Zealand active faults database. *New Zealand Journal of Geology and Geophysics* **59**, 86–96 (2016).
166. GNS. *New Zealand Active Faults Database*, <https://data.gns.cri.nz/af/> (2020).
167. AIST. Active Fault Database of Japan, February 28, 2012 version. *Research Information Database DB095*, https://gbank.gsj.jp/activefault/index_e_gmap.html (2012).

168. Allmendinger, R. W. & González, G. Invited review paper: Neogene to Quaternary tectonics of the coastal Cordillera, northern Chile. *Tectonophysics* **495**, 93–110 (2010).
169. Rubilar, J., Martínez, F., Arriagada, C., Becerra, J. & Bascuñán, S. Structure of the Cordillera de la Sal: A key tectonic element for the Oligocene-Neogene evolution of the Salar de Atacama basin, Central Andes, northern Chile. *Journal of South American Earth Sciences* **87**, 200–210 (2018).
170. Sepulveda, T., Cortes A, J., Melnick, D. & Cisternas, M. Neotectónica y paleosismología del cabalgamiento Andino Occidental (WAT) en la región del Maule, Chile Central, 36S. In *XV Congreso Geológico Chileno*. (2018).

Acknowledgements

We acknowledge financial support from the Millennium Nucleus CYCLO (The Seismic Cycle Along Subduction Zones) funded by the Millennium Scientific Initiative (ICM) of the Chilean Government grant NC160025, Chilean National Fund for Development of Science and Technology (FONDECYT) grants 1181479 and 1190258, and the ANID PIA Anillo ACT192169. TanDEM-X DEMs were provided by the German Aerospace Center (DLR) under Science Proposals GEOL0845, GEOL1209, GEOL1628, and GEOL0707. We thank Digimapas and Arauco for providing LiDAR data.

Author contributions

Conceptualization, compilation of previous studies and mapping: V.M., D.M.; mapping of new faults, fault system classification and main text writing: D.M.; figures preparation: V.M., D.M.; database preparation: V.M., M.C., D.M.

Competing interests

The authors declare no competing interests.

Additional information

Supplementary information The online version contains supplementary material available at <https://doi.org/10.1038/s41597-021-00802-4>.

Correspondence and requests for materials should be addressed to D.M.

Reprints and permissions information is available at www.nature.com/reprints.

Publisher's note Springer Nature remains neutral with regard to jurisdictional claims in published maps and institutional affiliations.



Open Access This article is licensed under a Creative Commons Attribution 4.0 International License, which permits use, sharing, adaptation, distribution and reproduction in any medium or format, as long as you give appropriate credit to the original author(s) and the source, provide a link to the Creative Commons license, and indicate if changes were made. The images or other third party material in this article are included in the article's Creative Commons license, unless indicated otherwise in a credit line to the material. If material is not included in the article's Creative Commons license and your intended use is not permitted by statutory regulation or exceeds the permitted use, you will need to obtain permission directly from the copyright holder. To view a copy of this license, visit <http://creativecommons.org/licenses/by/4.0/>.

The Creative Commons Public Domain Dedication waiver <http://creativecommons.org/publicdomain/zero/1.0/> applies to the metadata files associated with this article.

© The Author(s) 2021